Effect of Co substitution on the magnetic order in $Ca(Fe_{1-x}Co_x)_2As_2$ single crystals studied by neutron diffraction

K. Prokeš,[1,*] S. Mat'aš,[1] L. Harnagea,[2] S. Singh,[3] S. Wurmehl,[2] D. N. Argyriou,[1] and B. Büchner[2]

[1]*Helmholtz-Zentrum Berlin für Materialien und Energie, M-11, Hahn-Meitner Platz 1, D-14109 Berlin, Germany*

[2]*Leibniz-Institute for Solid State and Materials Research (IFW)-Dresden, D-01171 Dresden, Germany*

[3]*Indian Institute of Science Education and Research (IISER), Pune, Maharashtra 411008, India*

(Received 7 December 2010; revised manuscript received 26 January 2011; published 21 March 2011)

$Ca(Fe_{1-x}Co_x)_2As_2$ single crystals with a concentration $x = 0.032, 0.039, 0.051, 0.056$, and 0.063 were prepared and investigated by means of magnetic susceptibility and neutron diffraction combined with *in situ* electrical resistivity. The x-T phase diagram has been constructed. With increasing Co substitution, the anomaly marking the tetragonal to low-temperature orthorhombic structural phase transition temperature T_S, the antiferromagnetic phase transition temperature T_N, and the ordered magnetic moment gradually decrease. For samples with $0.039 \leqslant x \leqslant 0.056$, both transitions split and the T_N appears at increasingly lower temperatures than T_S. There is a small but finite difference between T_S determined upon cooling and warming. For samples with $x = 0.063$, no orthorhombic distortion and no long-range magnetic order is observed. For $x \geqslant 0.051$ superconductivity appears at low temperatures and the onset of the superconducting phase transition temperature T_{SC} decreases slightly with increasing Co content. For the limited concentration range $0.051 \leqslant x \leqslant 0.056$, both long-range antiferromagnetism and superconductivity coexist. Comparison with $Ba(Fe_{1-x}Co_x)_2As_2$ indicates a more abrupt disappearance of magnetic order in $Ca(Fe_{1-x}Co_x)_2As_2$. We find a direct correspondence between the magnitude of the ordered magnetic moment and the degree of orthorhombic splitting.

DOI: 10.1103/PhysRevB.83.104414 PACS number(s): 74.70.Xa, 61.50.Ks, 74.25.−q, 75.30.−m

I. INTRODUCTION

Iron, a prototype ferromagnetic material, is not supposed to be compatible with classical BCS-type superconductivity. Iron ferromagnetically aligned spin moments create a local magnetic field that would destroy any Cooper pairs. The announcements by Hosono *et al.*[1] about the existence of superconductivity in F-doped iron pnictide LaFeAsO and by Rotter *et al.*[2] of a similar observation in K-doped $BaFe_2As_2$ therefore came as a big surprise and initiated exceptional interest and feverish activity around the world that continues to date. Since this discovery, a large number of experimental and theoretical studies have been undertaken to reveal relationships among structure, magnetism, composition, and superconductivity (SC). The parent RFeAsO (R = rare earth) and $AEFe_2As_2$ (AE = Ca, Sr, Ba) compounds are not superconductors at ambient pressure but undergo structural and antiferromagnetic (AF) transitions.[3–6] Upon chemical doping[2,3,7] or under pressure,[8,9] the structural and magnetic transitions are suppressed and SC eventually appears. Early studies were made mainly on polycrystalline samples. However, advances in single-crystal growth in recent years have enabled more systematic studies that also include studies addressing the rather weak anisotropy of magnetic and transport properties.[10–14] Concerning the substitution of transition metal for Fe, a relative large number of studies dealing with cobalt substitutions in $Ba(Fe_{1-x}Co_x)_2As_2$[11–16] but few on $Sr(Fe_{1-x}Co_x)_2As_2$[17–19] and recently also $Ca(Fe_{1-x}Co_x)_2As_2$ single crystals exist[12,20–22] in the literature, probably due to preparation difficulties. At ambient pressure, undoped $CaFe_2As_2$ undergoes a first-order transition from a high-temperature tetragonal (T) phase ($ThCr_2Si_2$ structure) to a structure with orthorhombic (O) symmetry at $T_S = 166$ K concomitant with an AF transition.[6,23] In this contribution we report neutron diffraction results on several $Ca(Fe_{1-x}Co_x)_2As_2$ single crystals combined with magnetic bulk and *in situ* electrical resistivity measurements leading to the determination of basic structural and magnetic properties and to construction of an x-T phase diagram.

II. EXPERIMENTAL PROCEDURE

Single crystals of $Ca(Fe_{1-x}Co_x)_2As_2$ were grown in three steps. First, the precursor materials (CaAs, Fe_2As, and Co_2As) were prepared by reacting stoichiometric quantities of the constituents under vacuum at temperatures of less than 900°C. In the second step, stoichiometric quantities of precursors were grounded, pressed into pellets, and sealed in a quartz ampoule under vacuum. The ampoule was heated at temperatures up to 850°C. Finally, the sintered $Ca(Fe_{1-x}Co_x)_2As_2$ pellets and the Sn shots were loaded in an alumina crucible, together with a second catch crucible, and subsequently sealed in an evacuated quartz ampoule. The charge was heated up to 1090°C for 24 h and then slowly cooled down to 600°C, where the flux was decanted. Resulting platelet-like single crystals with a mass of between 20 and 200 mg were investigated for Co composition and possible residual Sn content using a scanning electron microscope (SEM Philips XL 30) equipped with an energy-dispersive x-ray spectroscopy probe (EDX) and a wavelength dispersive x-ray probe (WDX). It has been confirmed that, within the sensitivity of EDX, no inclusions of Sn exist in either of our crystals and that the average Co concentration measured over 16 to 25 spots on each used sample is generally somewhat lower than the nominal composition. The statistical error in the Co concentration determination is less than 0.3 atomic percent (at%), that is, well below the error limit of the EDX technique (1–2 at%). In the following, when addressing the Co concentration, we keep the experimentally determined values. Further sample

preparation and characterization details are given in the recent work by Harnagea *et al.*[22]

The field dependence of magnetization curves $M(T)$ at selected temperatures and the temperature dependence of the static magnetic susceptibility $\chi = M/H$, where H denotes the applied magnetic field, were measured on zero-field cooled samples in the temperature range 2–200 K using a SQUID magnetometer (Quantum Design) in fields up to 5.5 T applied along the [110] direction. No correction for the demagnetization factor was applied, however, the signal originating from the sample holder was carefully subtracted.

Neutron diffraction experiments were performed on the E4 double-axis diffractometer at the Helmholtz-Zentrum Berlin using a neutron wavelength of $\lambda = 2.44$ Å and a standard cryostat capable of reaching temperatures down to 1.7 K. Samples were attached by means of Teflon tape to an aluminium holder, with their c axis either parallel or perpendicular to the rotation axis of the diffractometer. The E4 diffractometer is equipped with a 20×20-cm position-sensitive detector that provides a diffraction image over a range of scattering angles (2θ) as the sample is rocked over a specified angular range (ω). This considerably simplifies the task of mapping the evolution of the scattering signal with temperature. Two $\lambda/2$ filters reduce residual higher-order wavelength contamination to a level of less than 10^{-4}. Each nuclear reflection was measured typically for about 15 min. Magnetic reflections, due to their lower intensity, were measured for 3–5 times longer. To extract integrated intensities, the individual scans were analyzed by fitting to Gaussian profiles. The appropriate scattering lengths and the standard, weighted Fe^{2+}/Co^{2+} magnetic form factors were used in the refinement. We also followed the intensities of representative nuclear and magnetic reflections as a function of temperature. The electrical resistivity for selected Co concentrations was measured *in situ* during the neutron diffraction measurements using a standard four-point ac method with electrical current applied approximately along the [110] direction.

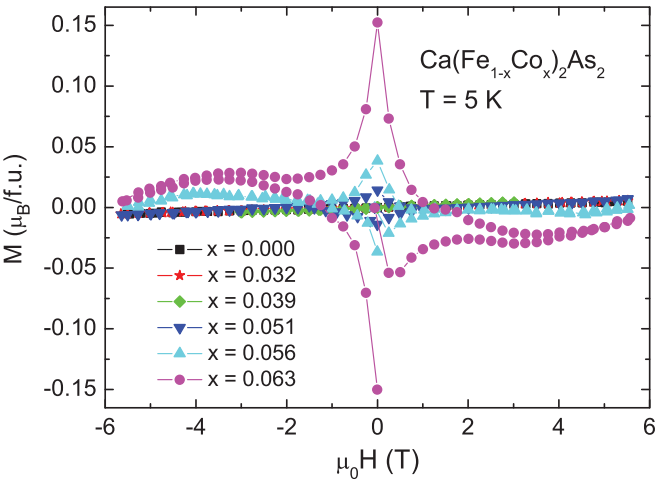

FIG. 1. (Color online) Magnetic field dependence of the magnetization measured at 5 K in fields of up to 5.5 T applied along the [110] direction on zero-field cooled $Ca(Fe_{1-x}Co_x)_2As_2$ samples.

III. RESULTS

A. Magnetization and magnetic susceptibility

In Fig. 1, the field dependence of the magnetization measured at 5 K with a field of up to 5.5 T applied along the [110] direction for various Co concentrations is shown. In all cases samples were first cooled down in zero field and then a field was applied. The magnetization remains positive for all samples with $x \leqslant 0.039$, also having a positive slope, which seems to increase with increasing x. For higher concentrations, however, one encounters a hysteretic behavior, typical for superconducting materials, which is combined with a paraprocess, giving rise to an increasingly positive slope at higher fields. The hysteresis increases with increasing Co concentration.

In Fig. 2 we show the temperature dependence of the magnetic susceptibility $\chi = M/H$ measured on zero-field cooled samples over a wide temperature range with a field of 1 T applied along the [110] direction for various Co concentrations. The magnetic susceptibility does not follow a Curie-Weiss law at high temperatures and remains very small but positive for samples with $x \leqslant 0.039$ over the whole temperature range. At high temperatures, a small drop in susceptibility values attributed to the appearance of an AF order below T_N can be seen. To show this phase transition in more detail, we show the magnetic susceptibility over a limited range of values. The anomaly broadens and T_N shifts upon increasing the Co substitution toward lower temperatures. For the $x = 0.063$ sample it is not discernible. At low temperatures, the magnetic susceptibility becomes diamagnetic for samples with $x \geqslant 0.051$ marking the onset of the SC state. The low-temperature detail of the temperature dependence of the magnetic susceptibility is shown in Fig. 3 and, on an expanded scale, in its inset. Although the transition becomes more pronounced and sharper with increasing Co concentration, the onset of the SC phase transition temperature T_{SC} shifts slightly toward lower temperatures.

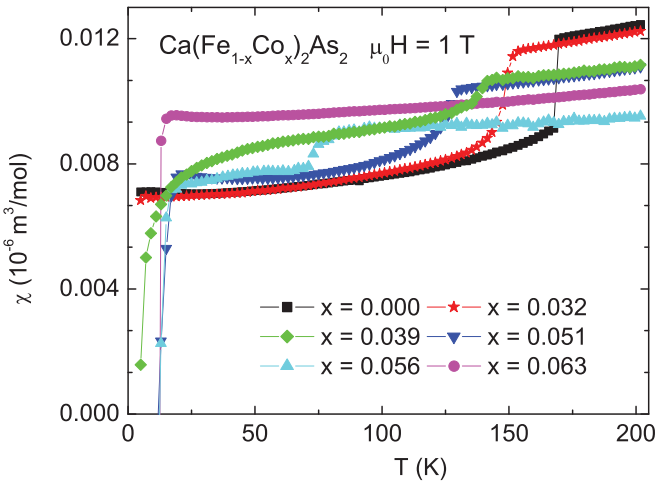

FIG. 2. (Color online) Temperature dependence of the magnetic susceptibility $\chi = M/H$ measured with a field of 1 T applied along the [110] direction on zero-field cooled $Ca(Fe_{1-x}Co_x)_2As_2$ samples.

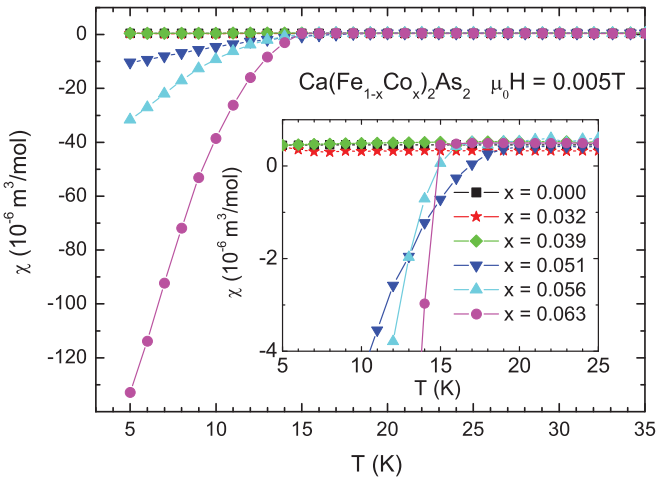

FIG. 3. (Color online) Low-temperature details of the dependence of the magnetic susceptibility measured with a field of 0.005 T applied along the [110] direction on zero-field cooled $Ca(Fe_{1-x}Co_x)_2As_2$ samples. Inset: Magnetic susceptibility in a limited range of values for various Co compositions.

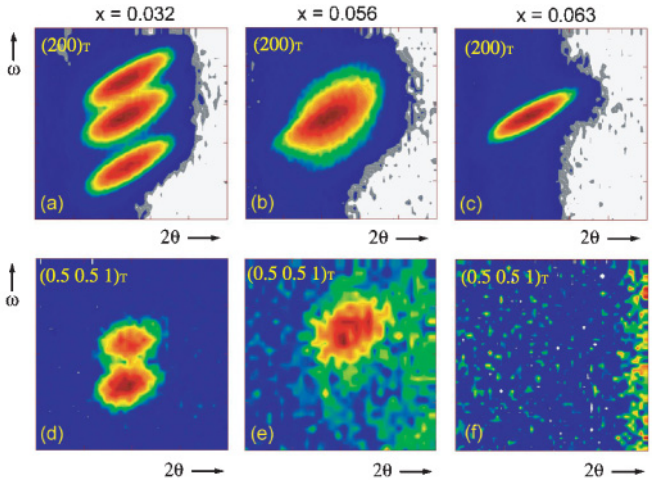

FIG. 4. (Color online) Color-coded diffraction maps showing the ω-2θ angular distribution of the diffracted neutron intensities recorded at the $(2\ 0\ 0)_T$ Bragg reflection positions for three selected $Ca(Fe_{1-x}Co_x)_2As_2$ samples, with (a) $x = 0.032$, (b) $x = 0.056$, and (c) $x = 0.063$ at 1.7 K. (d–f) Similar angular distributions of the diffracted intensities recorded under the same conditions for identical Co compositions at the magnetic $(0.5\ 0.5\ 1)_T$ reflection positions. Each panel represents a portion of data that covers 3.7° along 2θ and 3.1° along ω.

B. Neutron diffraction

Prior to neutron diffraction experiments at low temperatures, the samples were briefly checked and oriented using the neutron diffraction technique at room temperature. It was found that all the samples, irrespective of Co content, adopt a crystal structure at room temperature that conforms with the expected $ThCr_2Si_2$-type tetragonal structure with the space group $I4/mmm$. Although, as shown below, some of the investigated Co compositions do show the T-O structural phase transition, in this contribution we use systematic indexing within the high-temperature tetragonal notation. Figure 4 shows rocking curves through representative nuclear and magnetic reflection positions performed at 1.7 K on three $Ca(Fe_{1-x}Co_x)_2As_2$ samples, with $x = 0.032$, 0.056, and 0.063. The splitting of the $(2\ 0\ 0)_T$ Bragg reflection into three, well-separated reflections, as shown in Fig. 4(a), documents the presence of the O symmetry in this sample at 1.7 K. However, there are, in fact, four O-split Bragg reflections, belonging to four differently oriented O domains. For a given T reflection, two of the O reflections overlap and project on the same diffracted angles.[25] The splitting that appears below the T-O structural phase transition temperature T_S gradually decreases with increasing Co content, as evidenced by the rocking profile for the $x = 0.056$ sample shown in Fig. 4(b), and eventually disappears completely for the sample with $x = 0.063$, as shown in Fig. 4(c). For the latter and higher concentrations the system does not exhibit any T-O structural transition, preserving the high-temperature T crystal structure.

It has been unambiguously shown by using polycrystalline samples and single crystals[19] that the long-range AF ordering in all $AEFe_2As_2$ (AE = Ca, Sr, Ba) systems studied to date is below the Néel temperature T_N associated with the O structural phase. The original T crystal structure is distorted in such a way that the a-axis parameter gets slightly larger than the b-axis parameter. The measure of distortion, defined as $\delta = (a - b)/(a + b)$ is rather small, amounting typically to 0.5%–0.6%. The AF order in undoped $AEFe_2As_2$ (AE = Ca, Sr, Ba) systems is commensurate with the O structure (although some of the local probe experiments suggest an incommensurate AF order to be present in some systems)[16] and is built up from Fe moments directed along the longer orthorhombic a axis. Fe moments are coupled ferromagnetically along the b axis and antiferromagnetically along the a axis. The saturated moment ranges from 0.80 (2) μ_B for $CaFe_2As_2$[6,23] up to 1.00 (2) μ_B for the $SrFe_2As_2$ system.[23] The orientation of Fe moments along the longer a axis imposes that two of the four $(0.5\ 0.5\ 1)_T$ split magnetic reflections (corresponding to four structural domains) are extinct. This fact is documented for low temperatures in Figs. 4(d)–4(f), which show the diffracted neutron intensities for $Ca(Fe_{1-x}Co_x)_2As_2$ samples with $x = 0.032$, 0.056, and 0.063 at the magnetic $(0.5\ 0.5\ 1)_T$ Bragg reflection. For the former composition, two reflections are observed, suggesting that the type of AF order and the coupling between the Fe magnetic moments does not change upon doping with Co. Evaluation of the saturated magnetic moment residing on Fe ions leads to a value of 0.75 (4) μ_B, which is marginally smaller than the moment found for undoped $CaFe_2As_2$.[6] As the content of Co increases, the splitting gets smaller and, also, magnetic reflections eventually fade away. Due to the finite resolution of the E4 diffractometer, the two magnetic reflections merge into a single broad feature with a generally lower intensity for the $x = 0.056$ sample. The $x = 0.063$ sample shows no magnetic signal down to 1.7 K, suggesting either a loss of magnetism or a possibly different propagation of a magnetic structure. In the latter case, new magnetic Bragg reflections at other reciprocal space positions or an additional signal on top of nuclear refections (maybe the subject of sensitivity limitations) would be observed. However, an extensive search did not reveal any

additional magnetic signal. We can therefore conclude that for samples with $x \geqslant 0.063$, no long-range magnetic order with a magnetic propagation vector leading to new magnetic Bragg reflections exists, the AF being associated with the O phase. This result is completely in accord with magnetic susceptibility experiments described above suggesting a gradual loss of magnetism with increasing Co content.

Interestingly, for undoped $AE\mathrm{Fe_2As_2}$ (AE = Ca, Sr, Ba) samples the structural and magnetic phase transition temperatures coincide,[6,19,24,26–28] but in $\mathrm{Ba(Fe_{1-x}Co_x)_2As_2}$[17,19] and $\mathrm{Sr(Fe_{1-x}Co_x)_2As_2}$,[12,19] upon doping with Co, the two transition temperatures split, the T_N being shifted more rapidly with doping toward lower temperatures. Recent electrical resistivity and magnetic bulk measurements by Harnagea *et al.*[22] suggest that such a departure of T_S and T_N takes place also in $\mathrm{Ca(Fe_{1-x}Co_x)_2As_2}$. However, it is of paramount importance to verify this result also by means of microscopic experiments.

In Fig. 5(a), the temperature dependence of the integrated intensity across the $(2\ 0\ 0)_T$ reflection position measured for the $x = 0.032$ sample upon heating is shown. Two of the O-split reflection intensities remain nearly constant with increasing temperature up to 140 K, then decrease abruptly and, finally, merge at T_S into a single T reflection. The remaining two domains that are not distinguishable in our measurement start to grow significantly about 20 K below T_S, peak just below 150 K, and decrease sharply above this temperature. The intensity sum of all the reflections, which is much larger below T_S than that of the undistorted $(2\ 0\ 0)_T$ reflection, increases below 140 K only moderately and exhibits a sharp decrease above 140 K, with an inflection point at 151 K. Linear extrapolations of temperature dependencies below and above the critical temperature intercept at 153 (1) K, a value that we associate with T_S. The $(2\ 0\ 0)_T$ reflection, however, continues to decrease with increasing temperature even well above the T_S. This effect can be ascribed to the reduced quality of the crystal in the vicinity of the T_S leading to lower extinction and higher scattered intensities.[6] In Fig. 5(b) we show the temperature dependence of the integrated intensities of the two magnetic reflections associated with the $(0.5\ 0.5\ 1)_T$ reflection. As shown, their intensities decrease monotonically with increasing temperature and both reflections disappear at $T_N = 153$ (1) K. There is no increase in intensity just below 150 K as seen for the sum of two O structural domains. We can safely conclude that for the sample with $x = 0.032$, there is no significant difference between T_S and T_N. This is in clear contrast to the $\mathrm{Ba(Fe_{1-x}Co_x)_2As_2}$ system having the same level of Co concentration, which shows a clear difference between T_S and T_N by about 10 K.[32] From the angular positions of the split $(2\ 0\ 0)_T$ nuclear reflections and from the split of $(0.5\ 0.5\ 1)_T$ magnetic reflections, we have evaluated the δ parameter under the assumption that the twinning is solely caused by the difference in the lattice parameters upon the T-O phase transition. The resulting temperature dependencies determined from the nuclear reflections upon cooling and warming and and from magnetic reflections upon heating are shown in Fig. 5(c). The agreement between the nuclear and the magnetic dependence is excellent over the majority of the temperature range, except for the narrow region around T_S, where the δ parameter determined from magnetic reflections

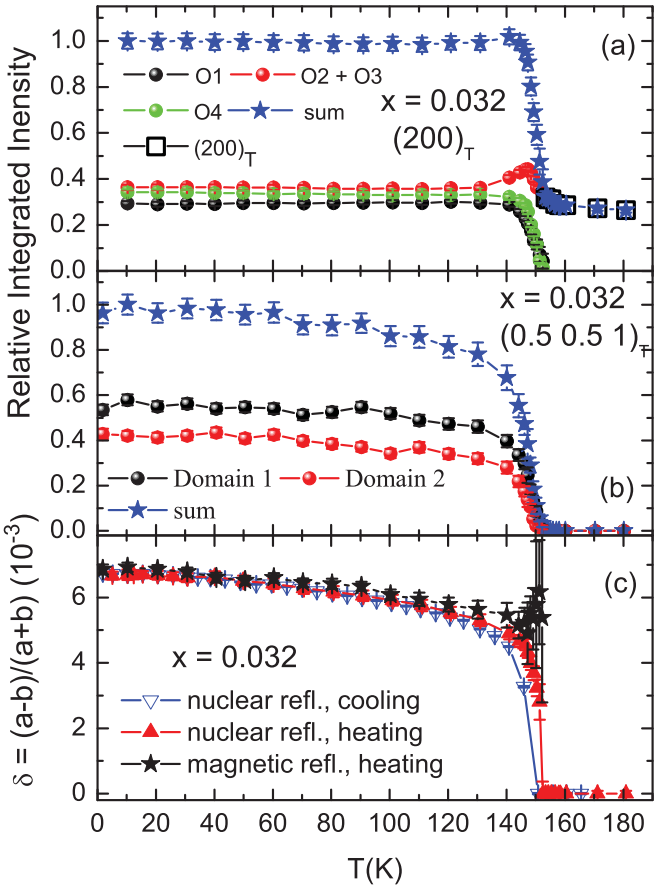

FIG. 5. (Color online) (a) Temperature dependence of the integrated intensity of the $(2\ 0\ 0)_T$ reflection (and the orthorhombically split reflections) measured for the $x = 0.032$ sample upon heating. (b) Temperature dependence of the integrated intensities of the two orthorhombically split magnetic reflections originating from the $(0.5\ 0.5\ 1)_T$ reflection upon heating. (c) Temperature dependencies of the splitting parameter $\delta = (a - b)/(a + b)$, calculated from the nuclear and magnetic reflections measured at increasing and decreasing temperature.

seems to be larger. As can also be seen, there is a small but finite difference between cooling and warming branches as determined from nuclear reflections suggesting that the transition is of the first-order type, in agreement with the literature.[19,22] However, the absolute value of the δ parameter, $6.7(1) \times 10^{-3}$, is larger for the $\mathrm{Ca(Fe_{1-x}Co_x)_2As_2}$, $x = 0.032$, sample than the corresponding value for the $\mathrm{Ba(Fe_{1-x}Co_x)_2As_2}$ compound assuming the same Co content.

In Fig. 6(a) we show the temperature dependence of the diffraction signal in the vicinity of the $(2\ 0\ 0)_T$ Bragg reflection, projected on the rocking angle ω, as measured on an $x = 0.039$ sample with increasing temperature. Figure 6(b) shows the temperature dependence of the signal recorded through the $(0.5\ 0.5\ 1)_T$ reflection upon heating. Although having different numerical labels, both dependencies are drawn to scale. As shown, the T_N, which is estimated to be $\approx$132 (2) K, is lower than the $T_S = 137$ (2) K. Thus, we encounter a splitting of the two transition temperatures upon doping with Co, similar to that for $\mathrm{Ba(Fe_{1-x}Co_x)_2As_2}$[17,19] and $\mathrm{Sr(Fe_{1-x}Co_x)_2As_2}$[12,19] compounds. Similarly to the data measured for the

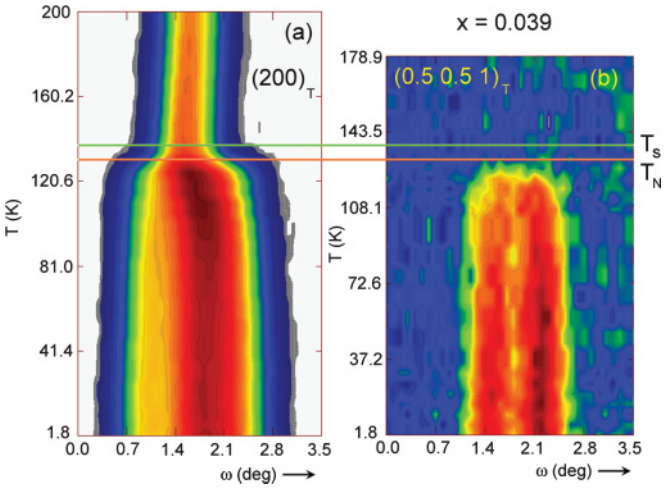

FIG. 6. (Color online) (a) Two-dimensional color map showing the temperature dependence of a portion of the diffraction pattern around the $(2\ 0\ 0)_T$ Bragg reflection position measured on a $Ca(Fe_{1-x}Co_x)_2As_2$ sample with $x = 0.039$ with increasing temperature. (b) Corresponding temperature development measured at the magnetic $(0.5\ 0.5\ 1)_T$ reflection position. Temperature scales for data were drawn to correspond to each other. The two solid lines denote the T_S and T_N phase transition temperatures.

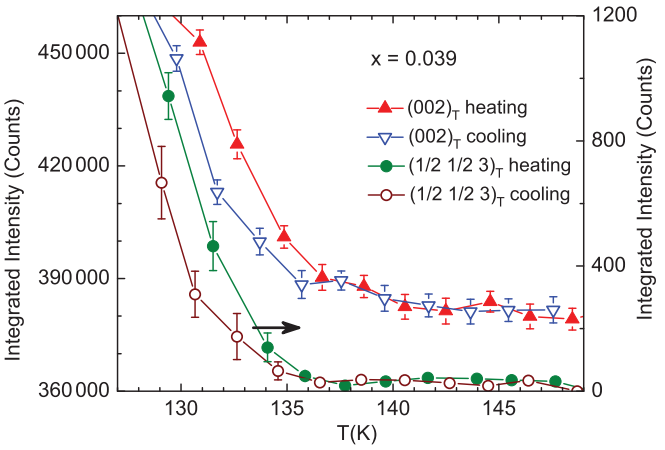

FIG. 7. (Color online) Temperature dependence of the integrated intensities measured at the $(0\ 0\ 2)_T$ and the magnetic $(1/2\ 1/2\ 3)_T$ Bragg reflection positions upon cooling and warming of the $Ca(Fe_{1-x}Co_x)_2As_2$ sample with $x = 0.039$ in the vicinity of the T_S and T_N phase transition temperatures.

$x = 0.032$ sample, also for the $x = 0.039$ concentration we observe a slight increase in the integrated intensity for the central O-split reflection but a monotonic decay for the remaining two and, also, for both magnetic reflections. The δ parameter inferred from the split of nuclear and magnetic reflections, $6.2(1) \times 10^{-3}$ is slightly smaller than that for the $x = 0.032$ sample. To study the structural and magnetic transitions in more detail, we followed the $(0\ 0\ 2)_T$ and $(0.5\ 0.5\ 3)_T$ reflections with cooling and warming. The resulting temperature dependencies of the integrated intensities are shown in Fig. 7. There is, again, a small, but clearly visible difference between the cooling and the warming branches, suggesting a first-order-type transition. Although the $(0\,0\,2)_T$ reflection suggests a T_S of 138 K, in agreement with measurements on the $(2\,0\,0)_T$ reflection, the magnetic reflection disappears completely only at 136 K, that is, about 3 K above the T_S inferred from the temperature dependence shown in Fig. 6(b). Closer inspection of the signal, however, suggests that this is due to the presence of short-range correlations just above T_N, which matches the linear extrapolation of the temperature dependence of the intensities to 0.

In Figs. 8(a) and 8(b) we show the temperature dependence of the integrated intensities of the $(2\ 0\ 0)_T$ and $(0.5\ 0.5\ 1)_T$ reflections measured upon heating of the $x = 0.051$ sample, respectively. Similarly to samples with $x = 0.032$ and 0.039, the integrated intensities of two of the O-split $(2\ 0\ 0)_T$ reflections first decrease slowly with increasing temperature and then decrease more rapidly when approaching $T_S \approx 130$ (3) K. The remaining central O-split $(2\ 0\ 0)_T$ reflection, which appears to be significantly more intense than the other two reflections, increases slowly up to about 125 K and then decreases sharply. The magnetic $(0.5\ 0.5\ 1)_T$ reflection, which appears, due to finite resolution, not to be split but significantly broadened, decreases over the whole temperature range monotonically and vanishes around $T_N = 120$ (4) K. Thus, we observe that the magnetic ordering disappears with increasing Co content at increasingly lower temperatures than the O-T structural transition, which shifts to lower temperatures too. The temperature dependence of the δ parameter calculated from the angular position of the nuclear reflection and the width of the magnetic reflection supposing the same intrinsic width as in the case of magnetic reflections observed for lower Co concentrations is shown in Fig. 8(c). Its absolute value of $5.8(1) \times 10^{-3}$ is clearly smaller than that for samples with a lower Co content.

Figures 9(a)–9(f), which shows color-coded diffraction maps across the $(2\ 0\ 0)_T$ and the $(0.5\ 0.5\ 1)_T$ reflection positions for the $x = 0.056$ sample at three selected temperatures, document the fact that for higher Co concentrations the magnetic order sets in at temperatures lower than those at which O distortion occurs. To exclude possible $\lambda/2$ contamination at the magnetic reflection position originating from (1 1 2) nuclear reflection, data taken at 120 K were subtracted from data shown in Figs. 9(d)–9(f). While at 85 K, that is, in the O distorted phase [see Fig. 9(c)], the magnetic Bragg reflection is clearly present [see Fig. 9(f)], it is missing at 95 K [see Fig. 9(e)], although at this temperature the $(2\ 0\ 0)_T$ reflection is still split [see Fig. 9(b)]. This can be seen by comparing its width with the measured width of the $(2\ 0\ 0)_T$ reflection in the tetragonal phase at 110 K, that is, above T_S [see Fig. 9(a)]. The residual intensity shown in Figs. 9(d) and 9(e) is due to critical scattering as seen in the case of the $x = 0.039$ sample (see Fig. 7) and, for example, in pure $BaFe_2As_2$.[29]

The subject whether the SC and AF phases are mutually exclusive or whether they can coexist in pure or doped $AEFe_2As_2$ (AE = Ca, Sr, Ba) systems is a greatly debated subject in the literature.[13,19,30,31] On the basis of neutron diffraction it has been shown that upon entering the SC state, the magnetic signal decreases in $BaFe_2As_2$ and $Ba(Fe_{1-x}Co_x)_2As_2$ systems.[13,19] At the same time, the orthorhombic distortion, manifested by the δ parameter, decreases.[32] In Fig. 10, which shows the temperature dependence of the magnetic reflection relative

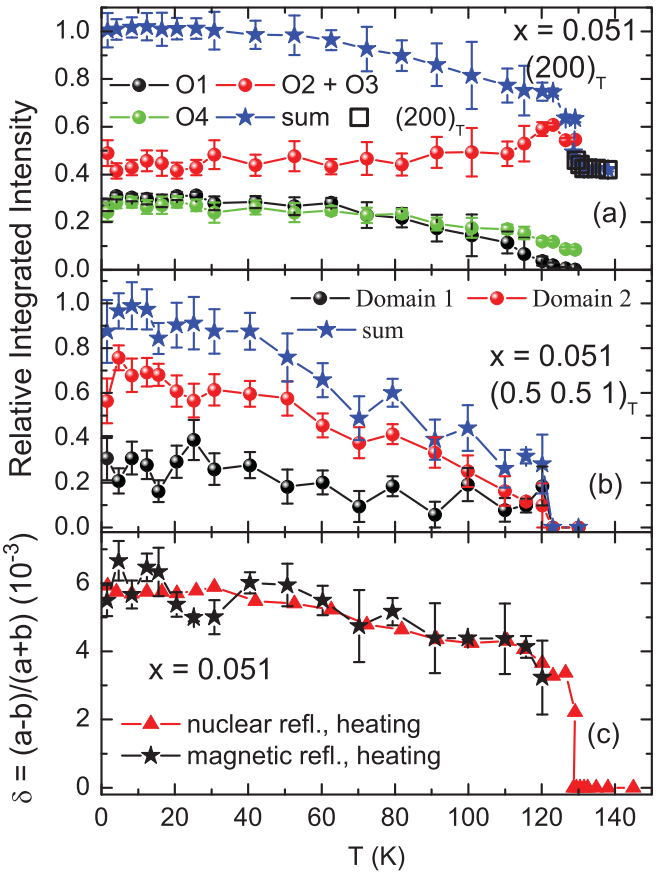

FIG. 8. (Color online) (a) Temperature dependence of the integrated intensity of the $(2\ 0\ 0)_T$ reflection, the orthorhombically split reflections originating from this reflection, and their sum measured using the $x = 0.051$ sample upon heating. (b) Temperature dependence of the integrated intensities of the two magnetic reflections originating from the $(0.5\ 0.5\ 1)_T$ reflection upon heating. (c) Temperature dependencies of the splitting parameter $\delta = (a - b)/(a + b)$, calculated from the above nuclear and magnetic reflections, measured with increasing temperature.

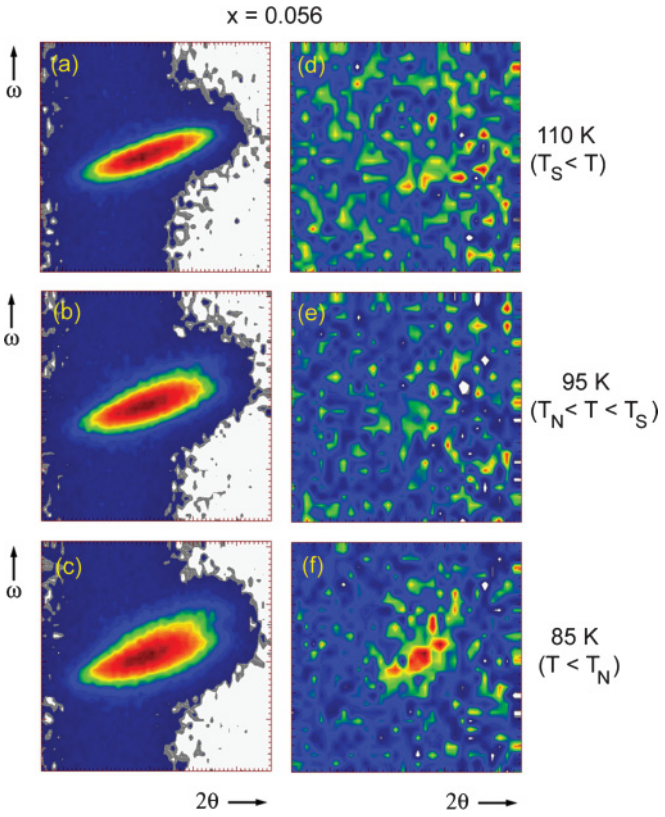

FIG. 9. (Color online) Color-coded diffraction maps showing the ω-2θ angular distribution of the diffracted neutron intensities recorded at the $(2\ 0\ 0)_T$ Bragg reflection position as measured on an $Ca(Fe_{1-x}Co_x)_2As_2$ sample with $x = 0.056$ (a) at 100 K (above T_S), (b) at 95 K (below T_S but above T_N), and (c) at 85 K (below T_N). (d–f) Similar angular distributions of the diffracted intensities recorded at the same temperatures at the magnetic $(1/2\ 1/2\ 1)_T$ reflection position. To exclude possible $\lambda/2$ contamination originating from (1 1 2) nuclear reflection, data taken at 120 K were subtracted in this case. Each panel represents a portion of data that covers 3.68° along 2θ and 3.1° along ω.

integrated intensities for the $x = 0.056$ sample together with the electrical resistivity measured *in situ* (normalized to the value at T_{SC}), we demonstrate that no bulk decrease in the magnetic order parameter exists for the $Ca(Fe_{1-x}Co_x)_2As_2$ system.

Thanks to the existing one-to-one correspondence between O-split magnetic and nuclear reflections, it is possible to calculate the magnetic moment for each of the O-split domains by normalizing the magnetic integrated intensities of the split $(0.5\ 0.5\ 1)_T$ reflection to the corresponding O-split nuclear reflections. In Fig. 11 we show the temperature dependencies of the magnetic moments determined for $Ca(Fe_{1-x}Co_x)_2As_2$ systems with various Co concentrations. For lower x values, the low-temperature moment values do not decrease significantly. However, for $x \geqslant 0.051$, a clear reduction occurs. This suggests a rather sudden loss of the magnetic moment with increasing Co content. Also, the temperature dependencies are rather unusual. The magnetic moment decreases for all concentrations with increasing temperature, first rather slowly. At a temperature of $0.9 \times T_N$ it still amounts to ≈80% of its low-temperature value. However, then it decreases very abruptly within a few kelvins. Above T_N, a negligible magnetic signal due to finite correlations is observed.

IV. THE *X-T* PHASE DIAGRAM

In Fig. 12(a), the x-T phase diagram constructed from our magnetic bulk measurements and neutron diffraction results, together with very few literature data,[6,19] is shown. For the pure $CaFe_2As_2$ system, the anomalies marking the tetragonal to low-temperature orthorhombic structural phase transition temperature T_S and the AF phase transition temperature $T_N \approx 169$ (1) K coincide. With increasing Co substitution both transitions decrease in temperature but, at first, remain undistinguishable. For samples with $0.039 \leqslant x \leqslant 0.056$, both transitions split and the T_N appears at increasingly lower temperatures compared to T_S. The saturated magnetic moment shown in Fig. 12(b), determined at 1.7 K, also decreases with increasing x: at first rather slowly, followed by a faster decay above $x = 0.039$. For a sample with $x = 0.063$, no orthorhombic distortion and no long-range magnetic order is observed. In Fig. 12(b) we also show the x dependence of the

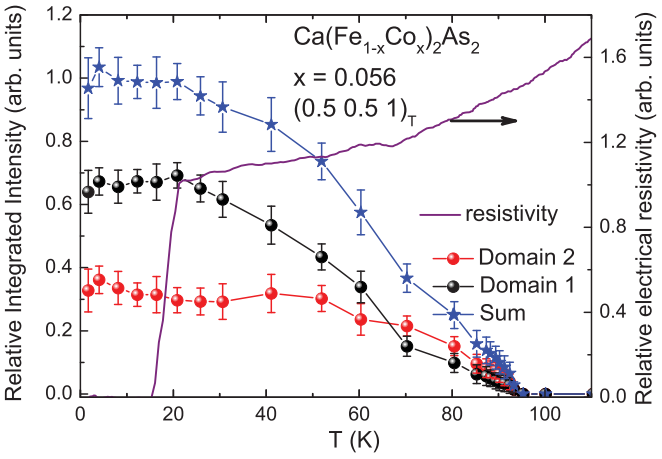

FIG. 10. (Color online) Temperature dependence of the relative integrated intensities of the two orthorhombically split magnetic reflections originating from the $(0.5\ 0.5\ 1)_T$ reflection measured upon heating for the $x = 0.056$ sample. *In situ* electrical resistivity measured simultaneously along the [1 1 0] direction and normalized to its value at the superconducting phase transition temperature is shown as well.

parameter $\delta = (a - b)/(a + b)$ calculated from the splitting of the nuclear reflections at 1.7 K. The inset in Fig. 12(b), showing the dependence of the magnetic moment on the δ parameter, suggests a direct linear correlation between the two quantities. In Fig. 12(a) we also show the concentration dependence of the onset of the superconducting phase transition temperature T_{SC} determined from the magnetic susceptibility. In this figure we also include the temperature at which the magnetic susceptibility for the $x = 0.039$ sample shows a downward curvature, although no sign of bulk SC is observed. In this case, the electrical resistivity does not drop to 0, suggestive of an SC transition only in a small portion of the sample volume, below a percolation limit. Indeed, magnetic susceptibility suggests that at this doping level, only a minute amount of SC phase exists in the sample. However, for $x \geqslant 0.051$, bulk SC with

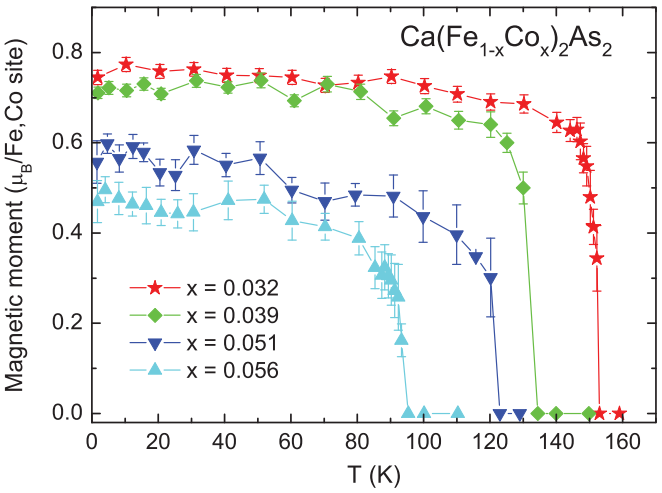

FIG. 11. (Color online) Magnitude of the magnetic moment per Fe/Co site as a function of the temperature of $Ca(Fe_{1-x}Co_x)_2As_2$ samples with various Co concentrations determined from neutron diffraction. Solid lines are guides for the eye.

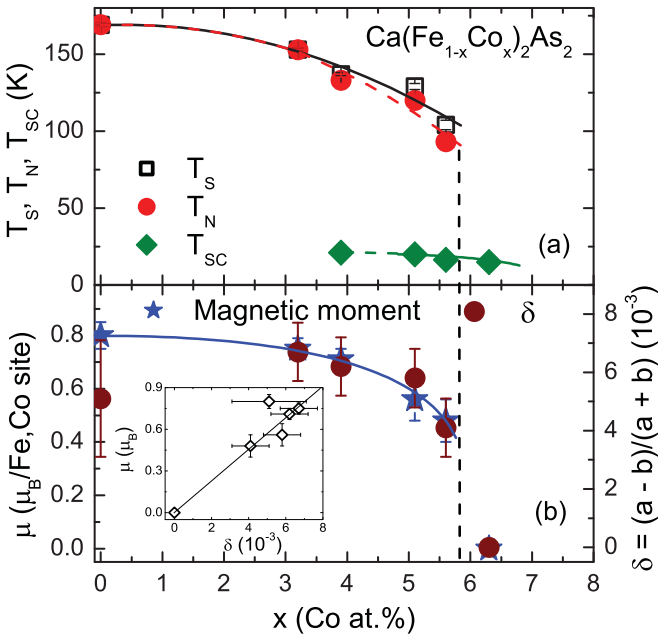

FIG. 12. (Color online) (a) x-T phase diagram of $Ca(Fe_{1-x}Co_x)_2As_2$ determined from magnetic bulk and neutron diffraction measurements showing the suppression of the structural and magnetic phase transition temperatures and the appearance of superconductivity at low temperatures upon increasing Co content$x$. (b) x dependence of the magnetic moment μ determined from neutron diffraction data at 1.7 K together with the splitting parameter δ calculated from the angular splitting of the nuclear reflections. Inset: Linear relation between μ and δ. The δ value for $x = 0$ is taken from Goldman *et al.*[6] Solid lines are guides for the eye; the vertical dashed line shows the approximate x concentration above which the magnetism in the $Ca(Fe_{1-x}Co_x)_2As_2$ system is lost.

zero resistivity appears at low temperatures and peaks at more than with 90 vol% for the optimally doped concentration $x = 0.063$.[22] The onset of the transition decreases slightly with increasing Co content. For the limited concentration range $0.051 \leqslant x \leqslant 0.056$, both long-range AF and SC exist. Interestingly, as noted by Harnagea *et al.*,[22] the onset of the SC transition as determined from the magnetic bulk measurements appears at lower temperatures than that determined from the electrical resistivity.

V. DISCUSSION AND CONCLUSIONS

All our data clearly suggest that upon increasing the Co substitution for Fe, the temperature range of the tetragonal crystal structure stability gets extended to lower temperatures. At the same time, the ordered moment decreases. This behavior seems to be a common feature for all the $AEFe_2As_2$ (AE = Ca, Sr, Ba) systems. There is a clear correspondence between the O distortion and the magnetic order, on one side, and the stabilization of the T crystal structure and appearance of an SC state at low temperatures, on the other, in all of these compounds. A strong coupling between the magnetic state of the Fe and the lattice in all the $AEFe_2As_2$ (AE = Ca, Sr, Ba) compound was recognized early on the basis of conventional electronic structure calculations.[33] However, the detailed temperature

dependencies are still remarkably different for the different groups. For $Ba(Fe_{1-x}Co_x)_2As_2$ compounds the suppression looks rather smooth, with a clear antagonism between the AF order and the SC state at low temperatures that even leads to an anomalous suppression of the O distortion for a small interval of Co concentrations[32] and a decrease in the scattered intensity due to AF order.[19] In contrast, our data clearly suggest that in $Ca(Fe_{1-x}Co_x)_2As_2$, a sudden collapse of magnetic order as measured both by magnetic bulk measurements and by neutron diffraction occurs. Our data are in good agreement with several recent works[20–22] but in clear disagreement with the work of Kumar *et al.*[12] suggesting that a sample with $x = 0.03$ is nonmagnetic with a considerable amount of the so-called paramagnetic phase. While the former fact cannot be explained easily without questioning the correctness of the Co concentration, the latter result is rather interesting, as it suggests the coexistence of several structural phases. In fact, this coexistence was observed previously for a pure $CaFe_2As_2$ system under quasihydrostatic[34] and uniaxial[35] pressure. It seems to be tempting to conclude that the extreme sensitivity of $CaFe_2As_2$ to pressure that is able even to transform the original T crystal structure to another structure [the so-called volume-collapsed tetragonal (cT) phase][36] with the same tetragonal symmetry, but with the c-axis lattice parameter smaller by 9%, could be responsible for the sudden loss of the O distortion and magnetism. This is supported by the concentration dependence of the c-axis lattice parameter, which is 1% smaller for $x = 0.15$ with respect to undoped $CaFe_2As_2$.[22] This decrease is larger than the decrease in the c-axis parameter upon Co substitution for the $Ba(Fe_{1-x}Co_x)_2As_2$ compounds, suggesting a much larger susceptibility to mechanical pressure for the former system, in agreement with pressure studies.[34,37]

It has been shown that in $CaFe_2As_2$ rather strong covalent Fe-As bonding exists[19,38] and that the calculated magnetic moment critically depends on the positional parameter of the As atoms, the only free structural parameter. When the experimental As atomic position is used in the calculations, the ordered Fe magnetic moments are calculated to be much larger than the experimental values, and the total energy of the compound is not at its minimum. If the total energy of a compound is minimized as a function of the As atomic position, a calculated Fe moment much closer to the experimental value is obtained. It is our working theory that the Co substitution causes subtle changes in the As atomic position that significantly affect the strength of the Fe-As covalent bonding and thus, also, the reduction of the ordered magnetic moment and the c-axis parameter. Unfortunately, our diffraction experiments were unable to determine the As positional parameter for different Co concentrations with enough precision to support this claim.

The temperature dependencies of integrated intensities of the O-split $(2\,0\,0)_T$ reflections show, for the central peak (that consists of two overlapping Bragg reflections originating from two O-split domains), an increase just below the T_S. This suggests that, for a certain temperature range that increases with increasing Co content, the T and the O phases coexist. This is also supported by the magnetic susceptibility measurements, which show a gradual broadening of the phase transition with increasing x and the claim by Kumar *et al.*[12] regarding the 40 vol% presence of a paramagnetic phase at low temperatures for $x = 0.03$ sample. Neutron diffraction experiments on $CaFe_2As_2$ under pressure[34,35] showed unambiguously that the sample is structurally multiphase, with traces of the T phase even at the lowest temperatures. We note that it has been shown that the suppression of the T_S phase transition and reduction in the As-Fe-As bond angle and Fe-Fe distance show the same behavior in $BaFe_2As_2$ under pressure as found in K-substituted samples.[39] At this stage we argue that upon increasing the Co content, the amount of the T phase increases at low temperatures, and eventually, for x larger than $\approx$0.06 the structure does not distort. The question is whether there is a direct link between orthorhombic distortion as a function of x and the microscopic distribution of Co atoms that might be nonuniform. Interestingly, 6% of Co atoms, which correspond to an exchange of every 16th Fe atom by Co atom, means that, on average, there is one Co for every four tetragonal crystallographic unit cells or two Co atoms per four orthorhombic crystallographic unit cells. Assuming a regular distribution, this translates into specific average interatomic distances between Co atoms of about 11 Å within the a-b plane and about 9.7 Å in directions outside the basal plane. We argue that these distances represent approximate critical values above which the covalent Fe-As and Fe-Fe bonding are significantly influenced and the T crystal structure stabilized. What remains is to explain the peculiar evolution of the distortion transition temperatures with increasing x. If our model is correct and Co atoms would be distributed without any positional variation, the value of the T_S would stay constant for concentrations lower than the critical concentration and the loss of orthorhombic distortion would be more sudden. Although the determination of the Co concentration using EDX did not revealed variation larger than 0.3 at%, it is clear that locally it can vary, leading to regions with either a higher or a lower concentration (and, correspondingly, with shorter or larger Co interatomic distances, respectively) than the critical distances mentioned above. This, in turn, would lead to regions in the crystal, with and without the O distortion at low temperatures. Because these regions are large, all the nuclear reflections are resolution limited at low temperatures (except for the $x = 0.056$ sample), the threshold critical Co concentration value has to be sharply defined. The initial rather small, and later much larger, suppression of T_S with increasing x is thus caused by small but finite variation of Co concentration. The irregularity in the x dependence of T_S and T_N seen in Fig. 12(a) is likely to be due to the finite absolute error of the EDX.

In conclusion, $Ca(Fe_{1-x}Co_x)_2As_2$ single crystals with $x =$ 0.032, 0.039, 0.051, 0.056, and 0.063 were investigated by means of magnetic bulk and neutron diffraction experiments combined with *in situ* electrical resistivity over a broad temperature range. With increasing Co content, the structural phase transition temperature T_S, from the tetragonal crystal structure with the space group $I4/mmm$ to the low-temperature orthorhombic structure with the space group $Fmmm$, decreases toward lower temperatures. The AF phase transition temperature T_N decreases as well and coincides for $x \leqslant 0.032$ with T_S. However, the originally sharp character of the structural transition is lost and the transition broadens significantly, indicating a range of temperatures where both T and O phases coexist. For higher Co concentrations both transitions split,

with T_N decreasing more rapidly, and eventually vanish for $x \geqslant 0.063$. Finite hysteresis of T_S upon cooling and warming suggests that the structural transition is of the first-order type. The ordered magnetic moment gradually decreases with increasing x. For samples with $x = 0.063$, no change in the crystal structure and no long-range magnetic order are observed down to 1.7 K. For $x \geqslant 0.051$, bulk SC appears at low temperatures. The onset of the SC transition temperature T_{SC} decreases with increasing Co content. The constructed x-T phase diagram suggests that for the limited concentration range $0.051 \leqslant x \leqslant 0.056$, both long-range AF and SC coexist. Comparison with $Ba(Fe_{1-x}Co_x)_2As_2$ indicates a more abrupt disappearance of magnetic order in $Ca(Fe_{1-x}Co_x)_2As_2$ with increasing x. Finally, we find a direct correspondence between the magnitude of the ordered magnetic moment and the degree of orthorhombic splitting.

ACKNOWLEDGMENTS

K.P. and D.N.A. acknowledge the Deutsche Forschungsgemeinschaft for support under the priority program SPP 1458 and Contract No. AR 613/1-2.

*Corresponding author: prokes@helmholtz-berlin.de

[1] Y. Kamihara, H. Hiramatsu, M. Hirano, R. Kawamura, H. Yanagi, T. Kamiya, and H. Hosono, J. Am. Chem. Soc. **128**, 10012 (2006).
[2] M. Rotter, M. Tegel, and D. Johrendt, Phys. Rev. Lett. **101**, 107006 (2008).
[3] Y. Ishida, F. Nakai, and H. Hosono, J. Phys. Soc. Jpn. **78**, 062001 (2009).
[4] P. C. Canfield, S. L. Bud'ko, N. Ni, A. Kreyssig, A. I. Goldman, R. J. McQueeney, M. S. Torikachvili, D. N. Argyriou, G. Luke, and W. Yu, Physica C **469**, 404 (2009).
[5] C. Krellner, N. Caroca-Canales, A. Jesche, H. Rosner, A. Ormeci, and C. Geibel, Phys. Rev. B **78**, 100504(R) (2008).
[6] A. I. Goldman, D. N. Argyriou, B. Ouladdiaf, T. Chatterji, A. Kreyssig, S. Nandi, N. Ni, S. L. Bud'ko, P. C. Canfield, and R. J. McQueeney, Phys. Rev. B **78**, 100506(R) (2008).
[7] A. S. Sefat, R. Jin, M. A. McGuire, B. C. Sales, D. J. Singh, and D. Mandrus, Phys. Rev. Lett. **101**, 117004 (2008).
[8] H. Takahashi, K. Igawa, K. Arii, Y. Kamihara, M. Hirano, and H. Hosono, Nature **453**, 376 (2008).
[9] M. S. Torikachvili, S. L. Bud'ko, N. Ni, and P. C. Canfield, Phys. Rev. Lett. **101**, 057006 (2008).
[10] M. J. Han, Q. Yin, W. E. Pickett, and S. Y. Savrasov, Phys. Rev. Lett. **102**, 107003 (2009).
[11] M. A. Tanatar, N. Ni, G. D. Samolyuk, S. L. Bud'ko, P. C. Canfield, and R. Prozorov, Phys. Rev. B **79**, 134528 (2009).
[12] N. Kumar, R. Nagalakshmi, R. Kulkarni, P. L. Paulose, A. K. Nigam, S. K. Dhar, and A. Thamizhavel, Phys. Rev. B **79**, 012504 (2009).
[13] N. Ni, M. E. Tillman, J.-Q. Yan, A. Kracher, S. T. Hannahs, S. L. Bud'ko, and P. C. Canfield, Phys. Rev. B **78**, 214515 (2008).
[14] D. K. Pratt, W. Tian, A. Kreyssig, J. L. Zarestky, S. Nandi, N. Ni, S. L. Bud'ko, P. C. Canfield, A. I. Goldman, and R. J. McQueeney, Phys. Rev. Lett. **103**, 087001 (2009).
[15] P. C. Canfield, S. L. Bud'ko, N. Ni, J. Q. Yan, and A. Kracher, Phys. Rev. B **80**, 060501(R) (2009).
[16] P. Bonville, F. Rullier-Albenque, D. Colson, and A. Forget, Euro Phys. Lett. **89**, 67008 (2010).
[17] A. Leithe-Jasper, W. Schnelle, C. Geibel, and H. Rosner, Phys. Rev. Lett. **101**, 207004 (2008).
[18] R. Khasanov, A. Maisuradze, H. Maeter, A. Kwadrin, H. Luetkens, A. Amato, W. Schnelle, H. Rosner, A. Leithe-Jasper, and H. H. Klauss, Phys. Rev. Lett. **103**, 067010 (2009).
[19] D. C. Johnston, Adv. Phys. **59**, 803 (2010).
[20] R. Klingeler, N. Leps, I. Hellmann, A. Popa, U. Stockert, C. Hess, V. Kataev, H.-J. Grafe, F. Hammerath, G. Lang, S. Wurmehl, G. Behr, L. Harnagea, S. Singh, and B. Büchner, Phys. Rev. B **81**, 024506 (2010).
[21] A. K. Pramanik, L. Harnagea, S. Singh, S. Aswartham, G. Behr, S. Wurmehl, C. Hess, R. Klingeler, and B. Büchner, Phys. Rev. B **82**, 014503 (2010).
[22] L. Harnagea, S. Singh, G. Friemel, N. Leps, D. Bombor, M. Abdel-Hafiez, A. U. B. Wolter, C. Hess, R. Klingeler, G. Behr, and B. Büchner (accepted for publication) .
[23] N. Ni, S. Nandi, A. Kreyssig, A. I. Goldman, E. D. Mun, S. L. Bud'ko, and P. C. Canfield, Phys. Rev. B **78**, 014523 (2008).
[24] H. Li, W. Tian, J. L. Zarestky, A. Kreyssig, N. Ni, S. L. Bud'ko, P. C. Canfield, A. I. Goldman, R. J. McQueeney, and D. Vaknin, Phys. Rev. B **80**, 054407 (2009).
[25] M. A. Tanatar, A. Kreyssig, S. Nandi, N. Ni, S. L. Bud'ko, P. C. Canfield, A. I. Goldman, and R. Prozorov, Phys. Rev. B **79**, 180508(R) (2009).
[26] J. K. Dong, L. Ding, H. Wang, X. F. Wang, T. Wu, G. Wu, X. H. Chen, and S. Y. Li, New J. Phys. **10**, 123031 (2008).
[27] J.-Q. Yan, A. Kreyssig, S. Nandi, N. Ni, S. L. Bud'ko, A. Kracher, R. J. McQueeney, R. W. McCallum, T. A. Lograsso, A. I. Goldman, and P. C. Canfield, Phys. Rev. B **78**, 024516 (2008).
[28] N. J. Curro, A. P. Dioguardi, N. ApRoberts-Warren, A. C. Shockley, and P. Klavins, New J. Phys. **11**, 075004 (2009).
[29] S. D. Wilson, Z. Yamani, C. R. Rotundu, B. Freelon, E. Bourret-Courchesne, and R. J. Birgeneau, Phys. Rev. B. **79**, 184519 (2009).
[30] I. I. Mazin, D. J. Singh, M. D. Johannes, and M. H. Du, Phys. Rev. Lett. **101**, 057003 (2008).
[31] R. M. Fernandes, D. K. Pratt, W. Tian, J. L. Zarestky, A. Kreyssig, S. Nandi, M. G. Kim, A. Thaler, N. Ni, P. C. Canfield, R. J. McQueeney, J. Schmalian, and A. I. Goldman, Phys. Rev. B **81**, 140501(R) (2010).
[32] S. Nandi, M. G. Kim, A. Kreyssig, R. M. Fernandes, D. K. Pratt, A. Thaler, N. Ni, S. L. Bud'ko, P. C. Canfield, J. Schmalian, R. J. McQueeney, and A. I. Goldman, Phys. Rev. Lett. **104**, 057006 (2010).
[33] K. D. Singh, Physica C **469**, 418 (2009).
[34] A. I. Goldman, A. Kreyssig, K. Prokeš, D. K. Pratt, D. N. Argyriou, J. W. Lynn, S. Nandi, S. A. J. Kimber, Y. Chen, Y. B. Lee, G. D. Samolyuk, J. B. Leão, S. J. Poulton, S. L. Bud'ko, N. Ni, P. C. Canfield, B. N. Harmon, and R. J. McQueeney, Phys. Rev. B **79**, 024513 (2009).
[35] K. Prokeš, A. Kreyssig, B. Ouladdiaf, D. K. Pratt, N. Ni, S. L. Bud'ko, P. C. Canfield, R. J. McQueeney, D. N. Argyriou, and A. I. Goldman, Phys. Rev. B **81**, 180506(R) (2010).

[36] A. Kreyssig, M. A. Green, Y. B. Lee, G. D. Samolyuk, P. Zajdel, J. W. Lynn, S. L. Bud'ko, M. S. Torikachvili, N. Ni, S. Nandi, J. B. Leao, S. J. Poulton, D. N. Argyriou, B. N. Harmon, R. J. McQueeney, P. C. Canfield, and A. I. Goldman, Phys. Rev. B **78**, 184517 (2008).

[37] R. Mittal, S. K. Mishra, S. L. Chaplot, S. V. Ovsyannikov, E. Greenberg, D. M. Trots, L. Dubronvinsky, Y. Su, T. Brückel, S. Matsuishi, H. Hosono, and G. Garbarino, Phys. Rev. B **83** 054503 (2011).

[38] K. D. Belashchenko and V. P. Antropov, Phys. Rev. B **78**, 212505 (2008).

[39] S. A. J. Kimber, A. Kreyssig, Y.-Z. Zhang, H. O. Jeschke, R. Valent, F. Yokaichiya, E. Colombier, J. Yan, T. C. Hansen, T. Chatterji, R. J. McQueeney, P. C. Canfield, A. I. Goldman, and D. N. Argyriou, Nat. Mater. **8**, 471 (2009).